small
NANO MICRO

Enhancing the Humidity Sensitivity of Ga_2O_3/SnO_2 Core/Shell Microribbon by Applying Mechanical Strain and Its Application as a Flexible Strain Sensor

Kewei Liu, Makoto Sakurai,* and Masakazu Aono**

The humidity sensitivity of a single β-Ga_2O_3/amorphous SnO_2 core/shell microribbon on a flexible substrate is enhanced by the application of tensile strain and increases linearly with the strain. The strain-induced enhancement originates from the increase in the effective surface area where water molecules are adsorbed. This strain dependence of humidity sensitivity can be used to monitor the external strain. The strain sensing of the microribbon device under various amounts of mechanical loading shows excellent reliability and reproducibility with a gauge factor of –41. The flexible device has high potential to detect both humidity and strain at room temperature. These findings and the mechanism involved are expected to pave the way for new flexible strain and multifunctional sensors.

1. Introduction

Flexible and stretchable electronics, a technology that integrates electronic devices on flexible substrates, is becoming one of the most interesting research fields owing to the low cost, wearability, and portability of devices based on such electronics.[1–7] In particular, flexible gas sensors have been realized on polymer substrates based on various materials, such as Si nanowire arrays,[8] ZnO nanorod arrays,[9] carbon nanotube films,[10–12] and metal nanotube arrays.[13] In addition to having the attractive properties of plastic substrates, including flexibility, a light weight, shock resistance, and softness, these flexible gas sensors also have high sensitivity and a rapid response.[8–13] Notably, in previous reports, the change in gas sensitivity induced by bending the substrate is very small and has thus always been ignored. This weak bending effect can be attributed to the loosely stacked structure of films and arrays, which usually counteracts the bending-induced strain and dissipates the strain energy. If we could fabricate a flexible gas sensor based on a single wire, tube or belt instead of a film or array, the tensile strain induced by bending the substrate would be directly applied to the single wire, tube or belt, and the strain-induced properties such as strain-dependent gas adsorption and strain-induced change of effective surface area could be studied. However, to the best of our knowledge, the effect of strain on the gas-sensing properties of a single wire, tube or belt has not been reported until now.

β-Ga_2O_3/amorphous SnO_2 core/shell microribbons have been fabricated by simple one-step chemical vapor deposition in our previous work.[14] These microribbons have fast and ultrahigh sensitivity to relative humidity (RH) around room temperature due to their unique structure, such as the large effective surface area of the amorphous SnO_2 shell and the core/shell heterojunction effect. Moreover, typical thermally switchable properties of β-Ga_2O_3/amorphous SnO_2 core/shell microribbons in wet air were demonstrated using a heating–cooling cycle between 20 and 30 °C. The ultrahigh sensitivity, fast response and recovery, and uniform granular surface of the amorphous SnO_2 shell of the humidity sensors suggest that the core/shell microribbon is one of the most promising candidates for the study of the effect of strain on the gas-sensing properties.

Herein, we investigate the effect of strain on the humidity-sensing properties of a single Ga_2O_3/SnO_2 core/

Dr. K. W. Liu, Dr. M. Sakurai, Prof. M. Aono
International Center for Materials Nanoarchitectonics (MANA)
National Institute for Materials Science (NIMS)
Tsukuba 305-0044, Japan
E-mail: Liukewei2007@yahoo.com.cn; Liu.Kewei@nims.go.jp; Sakurai.Makoto@nims.go.jp; Aono.Masakazu@nims.go.jp

DOI: 10.1002/smll.201201028

shell microribbon on a flexible substrate. The humidity sensitivity was enhanced by the application of mechanical strain. The reversible and reproducible strain dependence of the humidity-sensing properties indicates that the Ga_2O_3/SnO_2 core/shell microribbon can be used as an effective flexible strain sensor. Notably, the mechanism underlying the strain dependence is completely different from previously proposed mechanisms, that is, the piezoresistance effect, the metal–insulator transition effect, the change in Schottky barrier height (SBH) between semiconductor and electrodes, and the change in contact points between semiconductor nanowires, typically observed in ZnO nanowires,[15–17] Si nanoribbons,[18] VO_2 nanowires,[19] carbon nanotubes,[20–23] and graphene.[24,25] The performance of the device based on a single microribbon is evaluated and compared with that of other strain sensors.

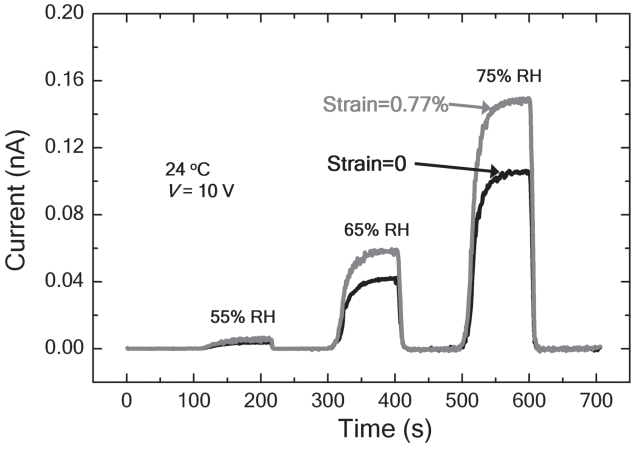

Figure 2. Dynamic responses of the flexible sensor to different levels of RH under 0 and 0.77% strain. The device was operated at 24 °C with an applied voltage of 10 V.

2. Results and Discussion

Microribbons were synthesized by simple one-step chemical vapor deposition, and typically had a width of 8–12 μm, a thickness of 1–2 μm, and a length of 5–9 mm.[14] Scanning electron microscopy (SEM) images and a schematic of a β-Ga_2O_3/amorphous SnO_2 core/shell microribbon are shown in **Figure 1**a. The microribbons have a well-defined core/shell structure with Ga_2O_3 in the core and SnO_2 in the shell. The thickness of the SnO_2 shell is approximately 300 nm and the shell has a very rough surface. A flexible device based on a single β-Ga_2O_3/amorphous SnO_2 core/shell microribbon was fabricated on a Kapton substrate (see Figure 1b). An as-grown microribbon was first transferred from the Si substrate onto a Kapton sheet. Then Au electrodes were fabricated by thermal evaporation through a shadow mask at room temperature. The thickness of the Au electrodes was approximately 500 nm, and the distance between the two electrodes was 200 μm. The Kapton substrate had a length of ≈1 cm, a width of ≈7 mm, and a thickness of 0.125 mm. When the substrate bends and stretches the microrod (see Figure 1b), tensile strain is induced in the β-Ga_2O_3/amorphous SnO_2 core/shell microribbon.[26]

The dynamic response of the flexible sensor to 55, 65, and 75% RH was characterized under 0 and 0.77% strain as shown in **Figure 2**. The measurement was carried out at 24 °C with an applied voltage of 10 V. In dry air (5% RH), the current of the device is under the instrumental limit (≈0.0001 nA). When humid air is introduced, the current increases by several orders of magnitude (e.g., ≈0.15 nA at 75% RH), thus indicating good humidity-sensing properties at room temperature. Interestingly, the current of the flexible device under 0.77% strain is larger than that without strain. This result indicates that tensile strain can markedly increase the humidity sensitivity. In other words, the current of the flexible device in humid air can be increased by applying tensile strain. This novel property can be used in flexible strain sensors.

To further investigate the effect of strain on humidity-sensing properties, the strain dependence of the electrical properties for the flexible sensor at 24 °C and 75% RH is shown in **Figure 3**. The inset in Figure 3a shows that the device can be bent very easily. The current–voltage (I–V) curves of the flexible device under different tensile strains are presented in Figure 3a. The linear I–V curves indicate the formation of ohmic contacts between the Au electrodes and the microribbon that are continuously maintained under different strains. With increasing tensile strain, the resistance of the device decreases continuously. Figure 3b shows the strain dependence of the relative change in current (defined as I_{strain}/I_0) at 24 °C and 75% RH when a fixed voltage bias of 10 V is applied to the flexible device. I_{strain}/I_0 as a function of strain shows linear behavior.

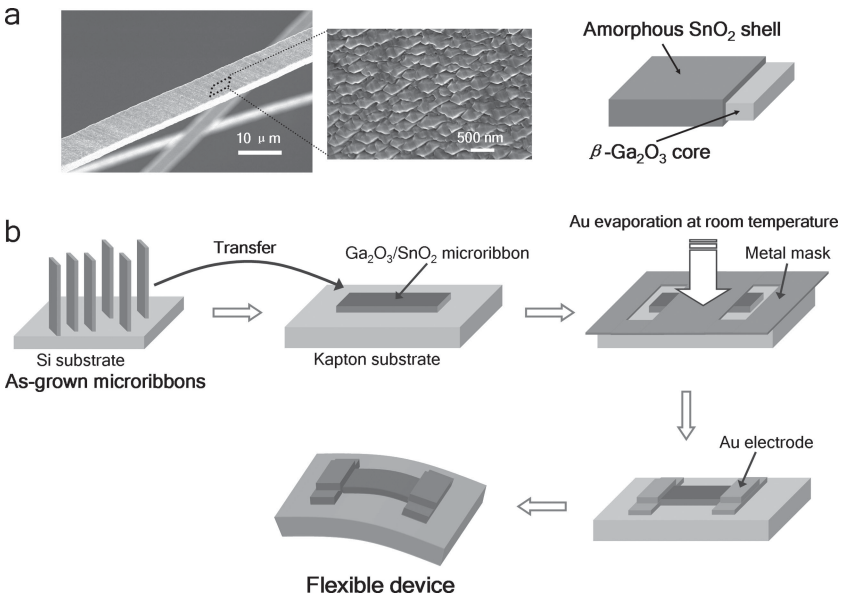

Figure 1. a) SEM images and schematic of β-Ga_2O_3/amorphous SnO_2 core/shell microribbon. b) Fabrication process of flexible device based on core/shell microribbon.

small 2012,
DOI: 10.1002/smll.201201028

small
NANO MICRO

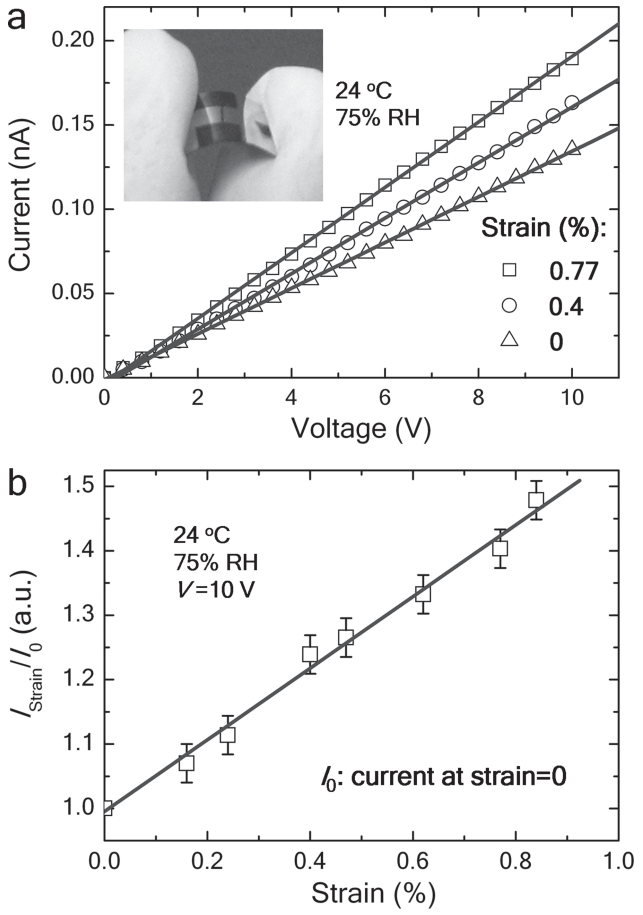

Figure 3. a) *I–V* curves of the core/shell microribbon-based flexible device under different strains at 24 °C and 75% RH. b) Relative change in current (defined as I_{strain}/I_0) as a function of strain.

To investigate the response and recovery properties of the flexible sensor to tensile strain, the current response to stepped and cyclic tensile loading is shown in **Figure 4**. The measurement was carried out under 10 V bias at 24 °C and

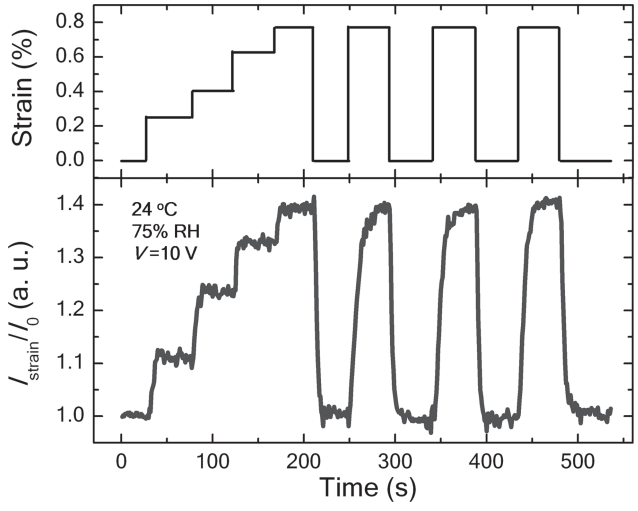

Figure 4. Response of the flexible sensor to tensile strain. The measurement was carried out under 10 V bias at 24 °C and 75% RH.

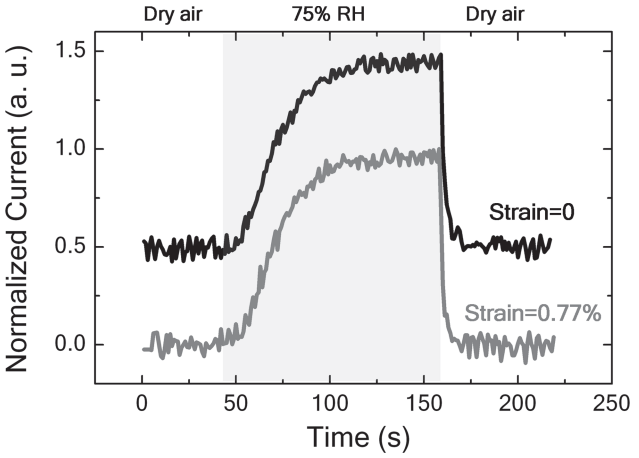

Figure 5. Normalized dynamic responses to 75% RH under 0 and 0.77% strain.

75% RH. We measured the current flow through the device after stretching the device step by step under 0, 0.24, 0.4, 0.62, and 0.77% strain (each strain was maintained for 40 s) and then alternating the strain between 0.77% and 0 every 80 s. It can be seen that the device has a relatively rapid response and recovery to the application and removal of strain. The current under strain was stable, and no significant change in current was observed after several loading cycles. To investigate the effect of strain on the dynamic response to humidity and its reversibility, the normalized dynamic response curves for the detection of 75% RH air under 0 and 0.77% strain were obtained (see **Figure 5**). Under both 0 and 0.77% strain, the response time and recovery time (defined as the time required to reach 90% of the final equilibrium value) were ≈40 and ≈10 s, respectively, when we switched the RH between 5 and 75%.

From Figures 3–5 it can be confirmed that the β-Ga_2O_3/amorphous SnO_2 core/shell microribbon on a Kapton substrate can be used as an effective flexible strain sensor in humid air at room temperature. The gauge factor (GF) is an important parameter for a strain sensor, which can be calculated using the formula:

$$\mathrm{GF} = \frac{\Delta R/R_0}{\varepsilon} = \frac{R_{\mathrm{Strain}} - R_0}{R_0 \times \varepsilon} \quad (1)$$

where ε is the strain applied to the sensor, R_0 is the initial resistance at zero strain, and R_{Strain} is the final resistance at a strain of ε. By fitting the experimental data (see the inset in **Figure 6**), the slope corresponds to the GF, which was calculated to be –41 for the device at 75% RH. The RH dependence of the GF is shown in Figure 6. It can be seen that the flexible sensor has an almost constant GF of about –41 between 40 and 75% RH. This indicates that the flexible strain sensor can be operated in a wide range of RH values.

To obtain a good understanding of the mechanism underlying the strain-sensing properties, a model based on the surface effect was proposed. The flexible sensor is in the insulating state in dry air (5% RH). When it is exposed to humid air, H_2O is physisorbed on the oxide surface and

DOI: 10.1002/smll.201201028

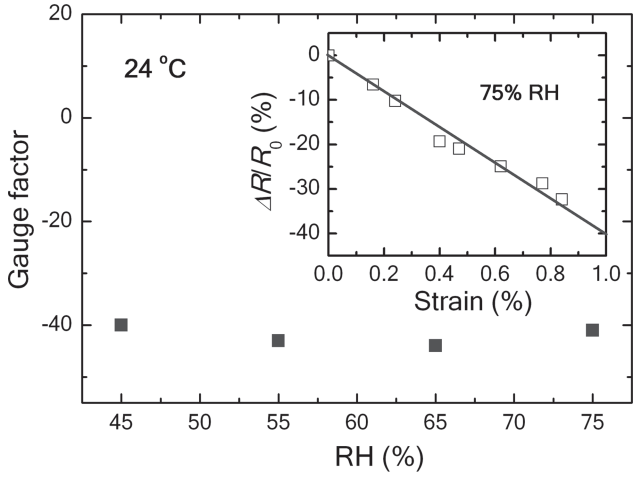

Figure 6. GF of the flexible sensor at RH values of 45, 55, 65, and 75%. The inset shows the relative change in resistance ($\Delta R/R_0$) as a function of the tensile strain at 75% RH. The slope corresponds to a GF of –41.

the conductivity of the sensor increases markedly. The current mainly flows near the rough surface of the amorphous SnO_2, as noted in our previous report.[14] When the substrate bends and stretches the microrod, tensile strain is induced in the β-Ga_2O_3/amorphous SnO_2 core/shell microribbon.[26] The values of strain given in this work were calculated using the equation

$$\varepsilon = \frac{\Delta L}{L} = \frac{t/2 + r/2}{R} \quad (2)$$

where L is the distance between the two Au electrodes, t is the thickness of the Kapton substrate (≈0.125 mm), r is the thickness of the β-Ga_2O_3/amorphous SnO_2 core/shell microribbon (≈1 μm), and R is the radius of curvature of bending. Owing to the bending and stretching of the microribbon, the strain may modify the surface of the amorphous SnO_2 in several different ways, which can be used to explain the mechanism of the novel strain sensor:

1) The surface chemistry of amorphous SnO_2 can be changed by applying strain, which strongly affects the adsorption and desorption of water molecules, and thus changes the conductivity of the device. However, because of the amorphous nature of the SnO_2 shell, the strain is mainly applied to the particle interface of the granular SnO_2 layer. Moreover, the strain-sensing properties have a weak RH dependence and the response time and recovery time are similar with and without the application of strain (see Figures 5 and 6). Therefore, the effect of the change in surface chemistry due to the application of strain can be neglected in this work.
2) The number of contact points between the semiconductors can be decreased by the application of tensile strain, which changes the conductivity of the device.[16] The reason for this is the reduced number of current channels. However, this strain-induced decrease in the number of contact points usually causes a decrease in conductivity. In our case, the tensile strain increases the current flowing in the flexible sensor (see Figures 2 and 3). Therefore, the effect of a strain-induced decrease in the number of contact points between amorphous SnO_2 grains can be excluded.
3) A strain-induced change in the band structure and the piezoelectric effect can change the Schottky barrier height between the semiconductor and electrodes, thereby resulting in a change in the resistance of the sensor.[15] As is well known, SnO_2 is a nonpiezoelectric material because of the inverse symmetry of its rutile structure. Additionally, the linear *I–V* curves indicate that the ohmic contacts are maintained, as shown in Figure 3a, which suggests that the electrical state of the semiconductors at the junction does not change under different strain conditions. Therefore, the piezoelectric effect can also be excluded. According to previous reports,[15,27] the band structure of semiconductors can be significantly affected by strain. In this work, the strain is mainly applied to the granular interface because of the amorphous nature of the SnO_2 shell. Moreover, no Schottky barrier can be found during the application of strain. Thus, the strain-induced change in the band structure of the SnO_2 shell can be neglected.
4) Gas-sensing properties depend on the effective surface area, because the amount of adsorption and desorption of a gas is proportional to the effective surface area of the device. As described previously,[14] the current flowing in the β-Ga_2O_3/amorphous SnO_2 core/shell microribbon under humid conditions is determined by three factors: the supply of electrons by the adsorption of water molecules, the current flowing in the SnO_2 shell due to the decrease in the depletion region, and the current flowing through the water layers on the surface. Bending and stretching can cause neighboring grains to separate slightly, and thus increase the effective surface area. Then, the contribution of water molecule adsorption to the surface conductivity becomes larger and the current flowing in the flexible sensor in humid air thus increases with increasing tensile strain. This increase in the effective surface area should be the main mechanism underlying the enhancement of humidity sensitivity. The mechanism can be confirmed by the decrease in humidity sensitivity under a compressive strain, which can reduce the effective surface area (see Figure S5, Supporting Information). Notably, since the SnO_2 shell has a rough surface and many particle interfaces, the increase in the effective surface area does not involve simple elongation such as that of a flat film.

On the basis of the above analysis, it can be concluded that the increase in the conductivity of the flexible sensor is caused by the strain-induced increase in the effective surface area in humid air. Finally, we compare the performances of our novel strain sensor with those of other strain sensors. **Table 1** shows the GF, the behavior of the $\Delta R/R_0$ versus strain characteristic, and the mechanism of strain sensors based on different materials. The GF of our sensor is approximately –41, which is smaller in magnitude than those of a single ZnO nanowire (–300 to 1300),[15] a ZnO nanowire/polystyrene film (116),[16] a single VO_2 nanobeam (100–350),[19] and a single carbon nanotube (200–300),[22,28] similar to that of a single Si

small 2012,
DOI: 10.1002/smll.201201028

NANO MICRO small

Table 1. Comparison between the performances of our flexible strain sensor and those of strain sensors based on other materials.

Material	GF	$\Delta R/R_0$ versus strain	Mechanism	Ref.
single ZnO nanowire	–300 to 1300	nonlinear	change in SBH	[15]
ZnO nanowire/polystyrene film	116	linear	change in contact points	[16]
ZnO – paper nanocomposite	21.12	linear	piezoresistance effect	[17]
graphene ribbons	–2	linear	–	[25]
	1.9	linear	change in band structure	[24]
single VO_2 nanobeam	100–350	nonlinear	metal– insulator transition	[19]
carbon nanotube polymer	10–20	linear	piezoresistance effect	[23]
single carbon nanotube	210	quasi-linear	change in bandgap	[22]
	269	linear	piezoresistance effect	[28]
single Si nanoribbon	43	linear	piezoresistance effect	[18]
single Ga_2O_3/SnO_2 core/shell microribbon	–41	linear	change in effective surface	this work

nanoribbon (43),[18] and larger than those of a ZnO–paper nanocomposite (21.12),[17] graphene ribbons (–2 or 1.9),[24,25] and a carbon nanotube polymer (10–20).[23] Our strain sensor has a previously unreported mechanism. Additionally, only our sensor and the single ZnO nanowire sensor in Reference [15] have a negative GF (note that the GF of the sensor based on graphene ribbons in Reference [25] is not in fact negative owing to the large prestrain in the original device).

3. Conclusion

Enhancement of the humidity sensitivity of a single β-Ga_2O_3/amorphous SnO_2 core/shell microribbon has been demonstrated by the application of mechanical tensile strain. This property was applied to fabricate a novel flexible strain sensor with a previously unreported mechanism: first, water molecules are adsorbed on the surface of the amorphous SnO_2 shell, which results in the surface conductivity; second, mechanical strain causes an increase in the effective surface area for the adsorption of water molecules, and thus produces enhancement of the conductivity. This flexible sensor can detect both humidity and strain with a rapid response and high GF at room temperature. We believe that these properties and the mechanism involved will pave the way for new flexible strain and multifunctional sensors.

4. Experimental Section

The β-Ga_2O_3/amorphous SnO_2 core/shell microribbons used in this study were synthesized by chemical vapor deposition.[14] A mixture of highly pure Ga_2O_3 powder (99.999%), SnO_2 powder (99.999%), and graphite powder (99.999%) with a weight ratio of 1:1:2 Ga_2O_3/SnO_2/C was used as the source. A ceramic boat containing the Ga_2O_3/SnO_2/C powder was placed in a horizontal tube furnace (see Figure S1, Supporting Information). The temperature was first increased to 200 °C in a vacuum, which was maintained for 10 min, to remove the water and adsorbed gas from the source. After that, the temperature was increased to 990 °C with a flow of highly pure argon mixed with 4% oxygen as the protective medium and carrier gas with a pressure of 9.0×10^2 Pa. This temperature was maintained for 60 min and then the furnace was naturally cooled to room temperature. The β-Ga_2O_3/amorphous SnO_2 core/shell microribbons grew at the end of the ceramic boat.

A microribbon was placed on a flexible Kapton substrate. Au was deposited through a shadow mask placed on the sample at room temperature. The *I–V* and gas- and strain-sensing characteristics of the β-Ga_2O_3/amorphous SnO_2 core/shell microribbon-based device were measured using a picoammeter (Keithley, model 6458) under different conditions (see Figure S2, Supporting Information).

Supporting Information

Supporting Information is available from the Wiley Online Library or from the author.

Acknowledgements

This work was supported in part by the World Premier International Research Center (WPI) Initiative on Materials Nanoarchitectonics, MEXT, Japan, and in part by JSPS KAKENHI (23560032).

[1] K. S. Kim, Y. Zhao, H. Jang, S. Y. Lee, J. M. Kim, K. S. Kim, J.-H. Ahn, P. Kim, J.-Y. Choi, B. H. Hong, *Nature* **2009**, *457*, 706.
[2] J. A. Rogers, T. Someya, Y. Huang, *Science* **2010**, *327*, 1603.
[3] D. J. Lipomi, M. Vosgueritchian, B. C.-K. Tee, S. L. Hellstrom, J. A. Lee, C. H. Fox, Z. N. Bao. *Nat. Nanotechnol.* **2011**, *6*, 788.
[4] Y. Sun, W. M. Choi, H. Jiang, Y. Y. Huang, J. A. Rogers, *Nat. Nanotechnol.* **2006**, *1*, 201.
[5] D. Y. Khang, H. Jiang, Y. Huang, J. A. Rogers, *Science* **2006**, *311*, 208.
[6] T. Sekitani, Y. Noguchi, K. Hata, T. Fukushima, T. Aida, T. Someta, *Science* **2008**, *321*, 1468.
[7] X. Lu, Y. Xia, *Nat. Nanotechnol.* **2006**, *1*, 163.
[8] M. C. McAlpine, H. Ahmad, D. Wang, J. R. Heath, *Nat. Mater.* **2007**, *6*, 379.
[9] J. Yi, J. M. Lee, W. I. Park, *Sens. Actuators B* **2011**, *155*, 264.
[10] Y. Wang, Z. Yang, Z. Hou, D. Xu, L. Wei, E. S.-W. Kong, Y. Zhang, *Sens. Actuators B* **2010**, *150*, 708.
[11] D. Fu, H. Lim, Y. Shi, X. Dong, S. G. Mhaisalkar, Y. Chen, S. Moochhala, L.-J. Li, *J. Phys. Chem. C* **2008**, *112*, 650.
[12] P.-G. Su, C.-T. Lee, C.-Y. Chou, K.-H. Cheng, Y.-S. Chuang, *Sens. Actuators B* **2009**, *139*, 488.
[13] M. A. Lim, D. H. Kim, C.-O. Park, Y. W. Lee, S. W. Han, Z. Li, R. S. Williams, I. Park, *ACS Nano* **2012**, *6*, 598.
[14] K. W. Liu, M. Sakurai, M. Aono, *J. Mater. Chem.* **2012**, *22*, 12882.
[15] J. Zhou, Y. Gu, P. Fei, W. Mai, Y. Gao, R. Yang, G. Bao, Z. L. Wang, *Nano Lett.* **2008**, *8*, 3035.

[16] X. Xiao, L. Yuan, J. Zhong, T. Ding, Y. Lin, Z. Cai, Y. Rong, H. Han, J. Zhou, Z. L. Wang, *Adv. Mater.* **2011**, *23*, 5440.
[17] H. Gullapalli, V. S. M. Vemuru, A. Kumar, A. Botello-Mendez, R. Vajtai, M. Terrones, S. Nagarajaiah, P. M. Ajayan, *Small* **2010**, *6*, 1641.
[18] S. M. Won, H.-S. Kim, N. Lu, D.-G. Kim, C. D. Solar, T. Duenas, A. Ameen, J. A. Rogers, *IEEE Trans. Electron Devices* **2011**, *58*, 4074.
[19] B. Hu, Y. Ding, W. Chen, D. Kulkarni, Y. Shen, V. V. Tsukruk, Z. L. Wang, *Adv. Mater.* **2010**, *22*, 5134.
[20] T. Yamada, Y. Hayamizu, Y. Yamamoto, Y. Yomogida, A. Lzadi-Najafabadi, D. N. Futaba, K. Hata, *Nat. Nanotechnol.* **2011**, *6*, 296.
[21] J. Zhang, J. Liu, R. Zhuang, E. Mader, G. Heinrich, S. Gao, *Adv. Mater.* **2011**, *23*, 3392.
[22] C. Stampfer, T. Helbling, D. Obergfell, B. Schoberle, M. K. Tripp, A. Jungen, S. Roth, V. M. Bright, C. Hierold, *Nano Lett.* **2006**, *6*, 233.
[23] K. Lee, S. S. Lee, J. A. Lee, K.-C. Lee, S. Ji, *Appl. Phys. Lett.* **2010**, *96*, 013511.
[24] M. Huang, T. A. Pascal, H. Kim, W. A. Goddard, J. R. Greer, *Nano Lett.* **2011**, *11*, 1241.
[25] Y. Wang, R. Yang, Z. Shi, L. Zhang, D. Shi, E. Wang, G. Zhang, *ACS Nano* **2011**, *5*, 3645.
[26] K. J. Lee, J. Lee, H. Hwang, Z. J. Reitmeier, R. F. Davis, J. A. Rogers, R. G. Nuzzo, *Small* **2005**, *1*, 1164.
[27] A. Alizadeh, P. Sharma, S. Ganti, S. F. LeBoeuf, L. Tsakalakos. *J. Appl. Phys.* **2004**, *95*, 8199.
[28] N.-K. Chang, C.-C. Su, S.-H. Chang, *Appl. Phys. Lett.* **2008**, *92*, 063501.

Received: May 11, 2012
Revised: June 12, 2012
Published online:

DOI: 10.1002/smll.201201028